Determination of Density Distribution in Spheroidal Colloidal Particles by Transmission Electron Microscopy

Igor Sevonkaev, Ionel Halaciuga, Dan V. Goia, Egon Matijević *
Center for Advanced Material Processing, Clarkson University, Potsdam, NY, 13699-1814

Abstract

The variation in the density distribution in spheroidal particles was evaluated by transmission electron microscopy (TEM) and quantified by image processing. Large silver spheres and gold nanoparticles were examined and compared to amorphous silica and acrylate-methacrylate polymer spheres. The latter can be considered as ideal homogeneous model samples. Image files having *.dm3 extension, obtained from TEM, were processed with ImageJ software, and later analyzed with script written in Microsoft Visual C++. It is shown that the radial density distribution of highly crystalline gold nanoparticles resemble the used models, while in larger polycrystalline silver particles it differs significantly from the "ideal" spheres. Deviations from linearity for gold and silver could be interpreted in terms of finite polydispersity and internal inhomogeneities.

Key words: Bulk Density Distribution, Gold Particles, Image Processing, Polymer Particles, Silver Particles.

Introduction

It is well known that many properties of finely dispersed matter (optical, magnetic, adsorptive, etc.) depend not only on chemical composition, but also on the size, shape, and internal structure of individual particles. For this reason in many applications it is important that the solids consist of entities as uniform as possible. While many methods are available for the preparation of well-defined nanometer to micrometer particles of different morphologies (1, 2, 3), their size distribution may vary somewhat, as well as the internal structure or some other properties. For example, the internal density of spheres may change from the center to the periphery, which could affect their optical, electrical, and thermo-mechanical characteristics. Therefore, it is desirable to have methods that could quantify such properties within individual particles.

This study describes an analytical method that allows detecting density variation due to internal inhomogeneity and particles size. For this purpose a transmission electron microscopy (TEM) technique was applied to determine the radial density distribution of individual metallic spheroids (silver and gold) and to compare both the theoretical and experimental values with those obtained for internally homogeneous spheres of silica and a polymer. The method is based on relationship (4):

$$log(I_0/I(r)) = \mu\rho x \tag{1}$$

where I_0 and $I(r)$ - are the incident and transmitted beam intensity, respectively, μ - is a quantity that involves experimental parameters, such as objective aperture and exposure conditions, ρ - is the material density, and x is the thickness of the sample. The plot of $I_0/I(r)$ as a function of x for an ideal sphere

* Corresponding author.
Email addresses: sevonkiv@clarkson.edu (Igor Sevonkaev,), matiegon@clarkson.edu (Egon Matijević).
URL: http://www.clarkson.edu/ sevonkiv (Igor Sevonkaev,).

should give a straight line. Indeed, the studied model systems produced such linear relationship, while deviations from linearity for gold and silver particles could be interpreted in terms of finite polydispersity and internal inhomogeneities. Thus, the method yields not only the bulk density data, but also qualitative indications on some physical properties of the dispersed systems.

Experimental

Materials

Silica particles were chosen due to their near perfect spherical shape and optimum contrast gradient when using bright field TEM (BFTEM). A dispersion of such particles, which were prepared by hydrolysis of tetraethyl-orthosilicate (TEOS) as originally described by Stöber (5) is illustrated in Fig. 1(a) (6). Two such particles of 200 nm were evaluated in the analysis (Fig. 1 (b)). The low polydispersity of silica spheres offered the possibility to confirm that the algorithm employed to determine that the radial density distribution was independent of size. The application of the model to larger spherical particles of lower specific gravity was verified with acrylate-methacrylate polymers of 3 μm in diameter (Fig. 2) supplied by CONPART (Oslo, Norway). The uniform gold nanoparticles (Fig. 3) were obtained by chemical precipitation in homogeneous solution to be described elsewhere. Polycrystalline spheroidal silver particles (Fig. 4), consisting of nanosize subunits were prepared by reduction of a silver-polyamine complex with iso-ascorbic acid as reported in (7). Essential properties of the materials are summarized in Table 1:

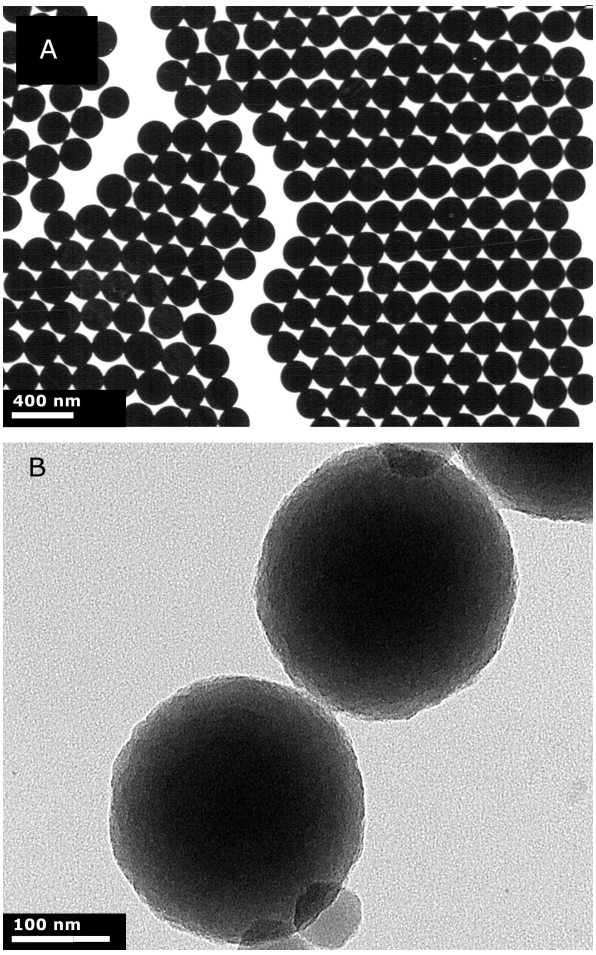

Fig. 1. a) Example of a dispersion of silica particles prepared by hydrolisys of TEOS (5, 6) b) TEM of two silica particles used in this study.

Table 1
Physical properties of particles.

Material	Specific Gravity, g/cm^3	Size, nm
Gold	19.3 (8)	20
Silver	10.6 (8)	50–10
Silica	2.2 (8)	100–200
Polymer	1.08 (9)	3000

Characterization methods

The samples for transmission electron microscopy (TEM) measurements were prepared by centrifuging the dispersions onto carbon coated copper grids (TED PELLA INC.) placed at the bottom of the tubes. The excess solvent was then removed and the grids were kept under vacuum overnight. Data were acquired by bright field TEM and elemental mapping in scanning transmission electron microscope (STEM) mode with a JEOL-2010 TEM instrument. Digital images, obtained with the Digital Micrograph software (GATAN INC.) and saved in *.dm3 format, allowed to store the relevant information needed in this study, such as exposure conditions, the incident and transmitted electron beam intensities, as well as the size of the pixels in units of length (e.g. nanometers).

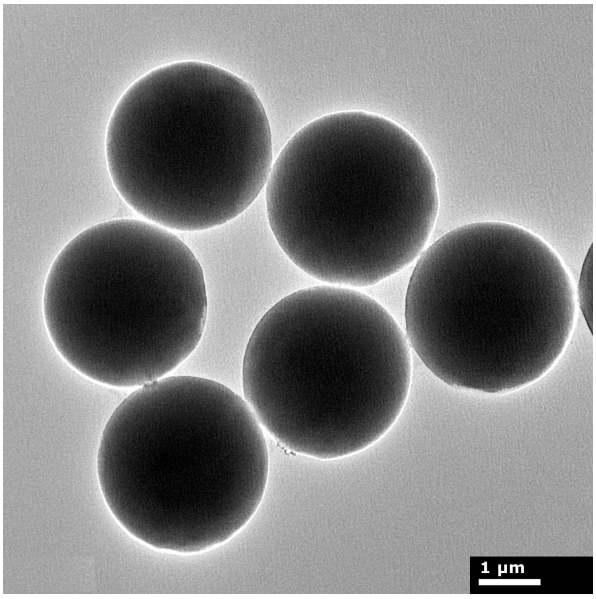

Fig. 2. TEM of acrylate-methacrylate polymer particles.

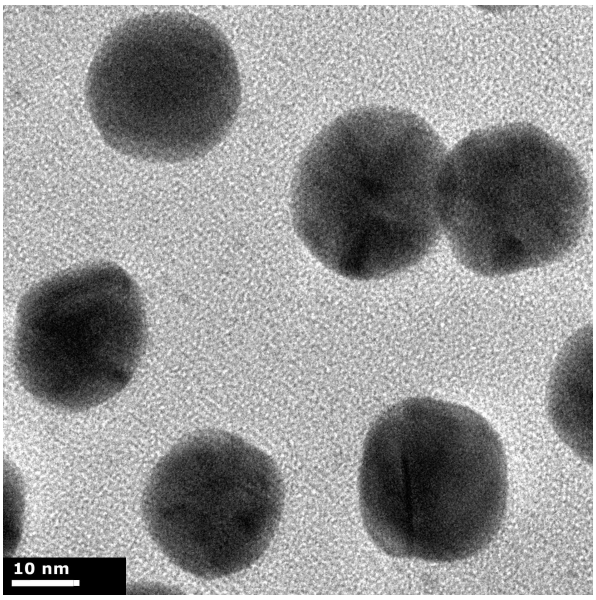

Fig. 3. TEM of nanosize gold particles prepared by chemical precipitation in homogeneous solution.

Data processing and interpretation

Digital images, acquired in bright field TEM mode, were evaluated using the ImageJ (image processing software (10, 11) as follows: a straight line was drawn from the approximate center of a particle towards the periphery (Fig. 5 single line). To avoid artifacts caused by angular variations of the intensities, a moderate thickness line was selected.

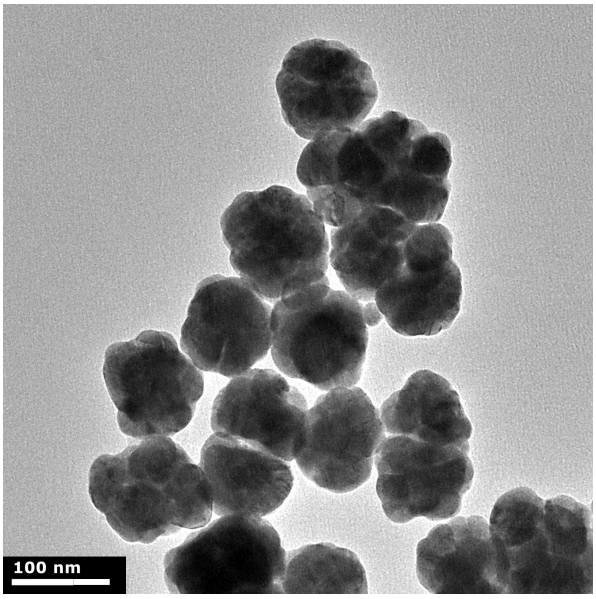

Fig. 4. TEM of nanosize silver particles prepared by reduction of silver-polyamine complex with iso-ascorbic acid according to (7).

Afterwards, a radial profile script using Microsoft Visual C++ programming language was implemented in the image processing software in order to perform the following tasks:

- identifying the background intensity that corresponds to I_0 in equation (1);
- dividing a particle into 36 equal angular segments (Figure 5 multiple lines);
- finding the particle's boundaries inside the built circumference, defining the average radius of the particle, and finding its geometrical center;
- constructing the intensity profile $I(r)$ along each line (Figure 6);
- calculating and storing of these values in data file (*.dat).

Information gathered with this script was arranged as follows: the lengths of the angular segments were stored in 36 columns, while the number of pixels along each radius was stored in rows (approximately 380-500 rows, depending on the image magnification). The so obtained two-dimensional array was further statistically analyzed with a Microsoft Visual C++ script by averaging all 36 columns for each row and fitting the data to a linear function, as examplified for silica particles in Fig. 7.

Information gathered with this script was arranged in the following manner: the lengths of the angular segments were stored in 36 columns, while the number of pixels along each radius was stored

in rows (approximately 380–500 rows depending on the image magnification), resulting in an array. Obtained matrix was further statistically analyzed with a Microsoft Visual C++ script by averaging all 36 columns for each row and fitting the data to a linear function, an example, for silica particles shown in (Figure 7).

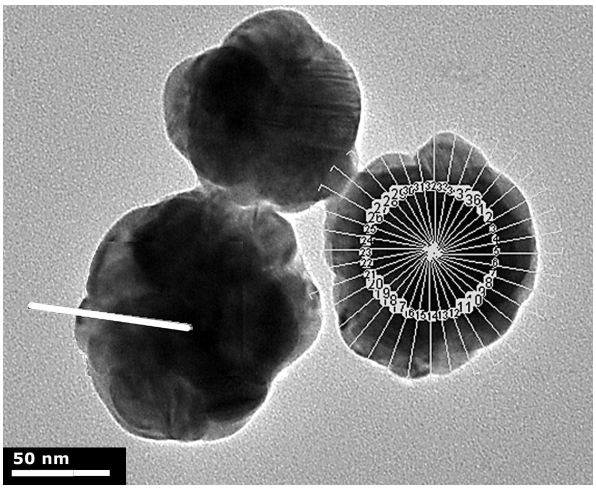

Fig. 5. Spheroidal silver particles, analyzed in ImageJ, with initial radial profile line of interest (single line on the left particle) and 36 angular segments (multiple lines on the right particle).

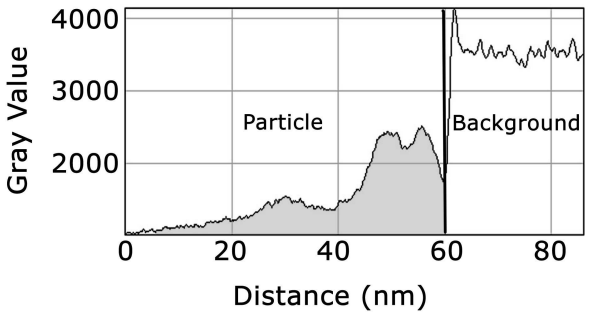

Fig. 6. Typical intensity profile from *.dm3 file along straight line taken from the center of a particle to beyond its boundaries.

Results

Since this study is mainly focused on the interpretation of digital images obtained by electron microscopy, taking advantage of the instrument output format was essential. Commonly, in imaging analytical techniques each pixel in an image is assigned to a measured intensity and the data are saved in various formats (e.g. $raw, jpg, tiff, bmp$, etc.). In most

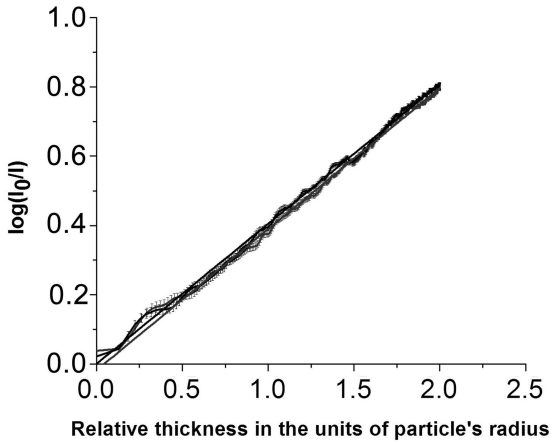

Fig. 7. The plot of data for silica particles density profile according to (1), with small oscillations near its average. Two curves represent two particles from Fig 1(b).

cases converted data lose some essential information because each pixel represents color values rather than absolute values of original intensity. For example, in a grayscale picture zero and 255 correspond to black and white pixels, respectively. Such conversion to grayscale maintains the general visual details and provides small file size, but lacks the ability to store specific details that might be needed for more advanced processing. For the purpose of this study the $*.dm3$ format was used (Fig. 6), because it stores pertinent information and eliminates the deficiency of a grayscale.

TEM images (Fig. 3 and 4) show that the metal particles investigates are not perfect spheres, but for processing purposes they were treated as such with equivalent radii as described in the radial profile script. The essential approximation, made in the script, considers 36 different radii (profiles) of a particle from the manually selected center to its edge with 10 degree increments (Fig. 5, multiple lines). Further, based on the calculated average radius, the script defines a confined circle and redefines the geometrical center of the particle. All further processing and interpretations are performed over the particle circumference generated in the last step. Using the described procedure, it was possible to obtain an appropriate contrast gradient of the systems summarized in Table 1 using apertureless bright field TEM mode.

The reference spherical silica and polymer particles showed gradual increase in transparency from the center to the periphery, while the transparency remained constant upon rotation with respect to the

center of symmetry. It is essential to recognize that even these "ideal" particles may have some minor surface roughness.

The profiles of bulk density of two individual silica particles (Fig. 7) follow the straight line as predicted by equation 1 for the sphere. Analogous results were obtained for the spherical acrylate-methacrylate particles as displayed in Fig. 8.

Nanosize gold investigated under BFTEM mode shows similar trends (Fig. 9) as the model systems. While the individual density profile of each sphere deviates slightly from linearity, the calculations show that the linearity improves, if one builds a stack of five individual entities (Fig. 10). This finding yields the same kind of density profile as for "ideal" silica particles.

In contrast, the same analysis, applied to the silver dispersion, shows considerably greater deviation (Fig. 11) in linearity than the other investigated cases. Furthermore, stacking of several silver particles lessens the profile deviation, but still does not produce reasonable linearity (Fig. 12).

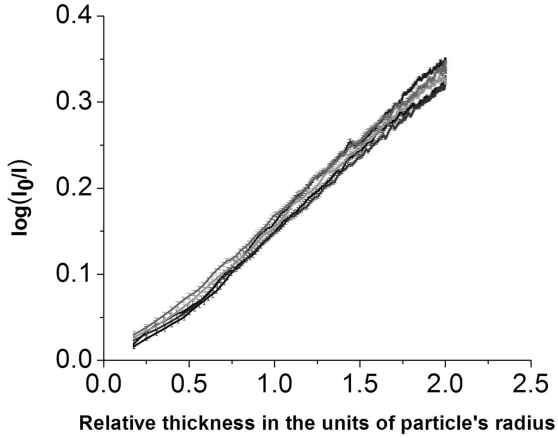

Fig. 8. The density profile plot data for five acrylate-methacrylate particles from Fig. 2.

Discussion

The results of the described analytical method are applicable to particles of any shape, but the program developed in this study can be employed only to spheroids. In principle, the data obtained are affected by the size and uniformity of the particles, their density, and internal structure. In this study the method was tested on rather uniform amorphous spheres of different size (i.e. silica and

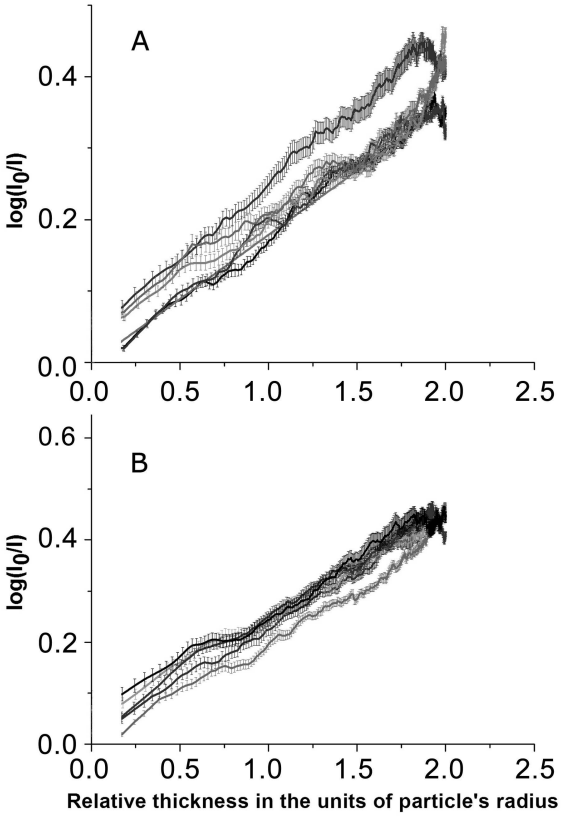

Fig. 9. a) A batch of five gold particles and b) data from another batch of five particles.

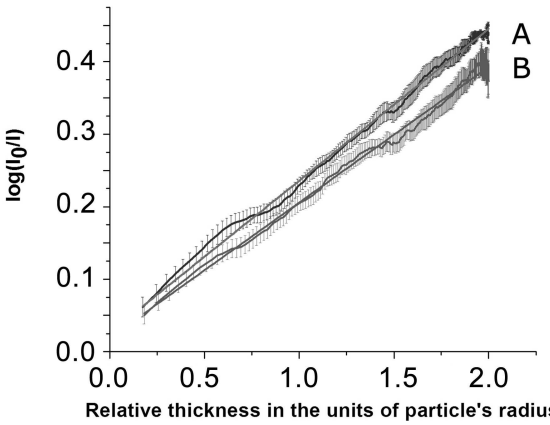

Fig. 10. Averaging of five particles from Fig. 9(a) and Fig. 9(b).

acrylate-methacrylate), and two metals of lesser shape uniformity and different internal compositions (i.e. gold and silver). The results of the analysis are expressed in plots as log of intensity ratios vs. particle's thickness, which in an ideal case

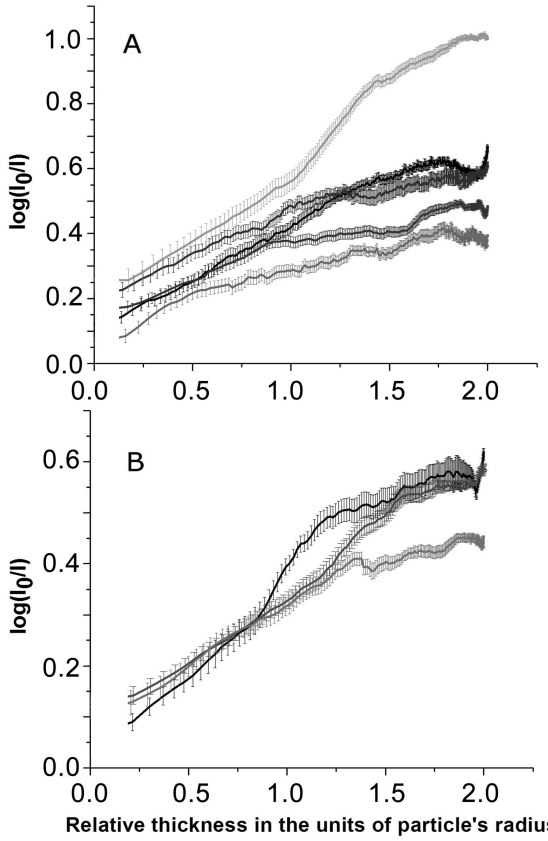

Fig. 11. a) A batch of five silver particles and b) data from another batch of three particles.

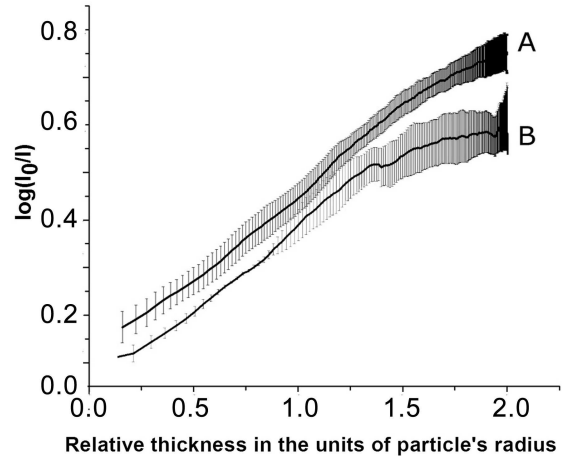

Fig. 12. a) STEM mode of nanosize silver particles of the same sample as in Fig. 4 and b) is their mapping equivalent.

should be linear as required by equation 1. In real systems the shapes of these plots can be used to qualitatively assess certain particle properties in a given dispersion. Thus, ideal spheres of somewhat different sizes generate the same profile with the same slope but there is a shift in vertical position. The magnitude of such shifts is indicative of the degree of polydispersity. Indeed, two model systems (i.e. silica and acrylate-methacrylate) yielded quite linear plots with relatively small vertical shifts, indicating their size uniformity (Fig. 7 and 8).

Departure from the linearity depends on internal inhomogeneity of the particles, caused either by crystal planes at high resolution, or their composite nature, such, when they are made up of smaller subunits. In the case of gold (Fig. 9) there is some deviation from linearity and more pronounced vertical shifts. While these particles are single crystals, the observed trends are partially due to some distortion of sphericity and to internal crystal planes. Averaging data for five particles (Fig. 10) eliminates the structural and morphological effects.

Finally, silver particles show significant departure from the ideal case. It has been established that the experimental procedure [7] yields individual silver particles to consist of aggregates of smaller subunits. Obviously, their internal structure is responsible for the observed analytical results. Averaging data for five particles (Fig.12 plot B), similarly to gold, eliminates both internal effects and shape deviation from the ideal model. In contrast, using only three particles it is insufficient to obtain density profile for the entire silver dispersion (Fig. 12 plot A).

A final comment refers to the reproducible deviation from the linearity in density profile plot of silica particles between abscissa values of 0.25 and 0.5 (Fig. 7). The latter corresponds to distances of $0.96R$ and $0.98R$ from particle's center, where R is the averaged radius of a spheroidal particle. Such deviation can be caused by Fresnel diffraction at the edge of a sphere with high curvature. Fok (12) described the theoretical possibility of this phenomenon for the case of spherical objects that have a radius much larger than the wavelength of the incident radiation. Analogues effect was not observed with metallic particles investigated, because it was obscured by stronger deviation from linearity of their density profiles.

In principle, the density profile in a given particle can also be obtained by X-ray elemental mapping in the STEM mode. However, as shown in Fig. 13, this technique was unable to provide accurate results, due to poor resolution and high scattering blurriness in the images.

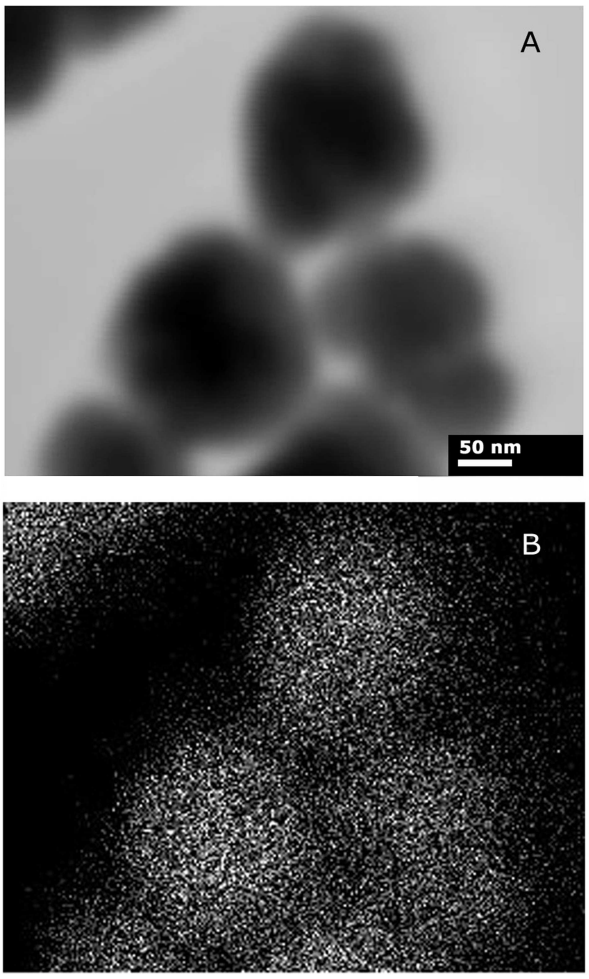

Fig. 13.

Conclusions

This study describes a model that can yield bulk density changes of spheroidal particles of different sizes and internal compositions from TEM images. Two amorphous spherical particles (organic acrylate-methacrylate and inorganic silica) yielded linear profile of bulk density from their center to periphery. In contrast, spheroidal particles of two metals (silver and gold) showed significant deviations of their density profiles due to shape and internal structure factors. However, assuming layers of several particles the density profile approaches the predicted linearity. This particular consequence may be important for applications, where film thickness properties are critical. Thus, applying the described method one may assess the particle packing in the deposition of thin layers in microelectronic and sensors.

Results with silver are of additional interest, because it has been now well established that a large number (if not most) uniform colloidal particles, prepared be precipitation, consist of smaller subunits **?**). Indeed, a model was developed that defines conditions under which monodispersed spheres can form by such aggregation mechanism (13, 14, 15).

Acknowledgements

The authors thank Mr. Morrow for providing gold nanoparticles, Prof. V. Privman and Dr. D. Robb for useful discussions and comments, and acknowledge the support from NSF under grant DMR-0509104.

References

[1] T. Sugimoto (Ed.), Fine Particles: Synthesis, Characterization, and Mechanisms of Growth (Surfactant Science), CRC, 2000.

[2] E. Matijevic, Preparation and properties of uniform size colloids, Chem. Mater. 5 (1993) 412–426.

[3] E. Matijevic, Uniform colloid dispersions - achivements and and challenges, Langmuir 10 (1994) 436–450.

[4] S. Daisuke, O. Tetsuo, Analytical Electron Microscopy for Materials Science, Springer, 2002.

[5] W. Stöber, A. Fink, E. Bohn, Controlled growth of monodisperse silica spheres in the micron size range., J. Colloid Interface Sci. 26 (1968) 62.

[6] W. P. Hsu, R. Yu, E. Matijevic, Paper whiteners: I. titania coated silica., J. Colloid Interface Sci. 156 (1993) 56.

[7] I. Halaciuga, D. Goia, Preparation of silver spheres by aggregation of nanosize subunits, J. Mater. Res. 26 (6) (2008) 1776–1784.

[8] R. C. Weast, Handbook of Chemistry and Physics, The Cmemical Rubber Co., 1968.

[9] D. O. Kipp, Plastic Material Data Sheets, MatWeb - Division of Automation Creation, Inc., 2004.

[10] M. Abramoff, P. Magelhaes, S. Ram, Image processing with imagej, Biophotonics International 11 (7) (2004) 36–42.

[11] W. Rasband, Imagej, U. S. National Institutes of Health, Bethesda, Maryland, USA, http://rsb.info.nih.gov/ij/.

[12] V. A. Fok, Fresnel diffraction from convex bodies, Uspekhi Fizicheskikh Nauk 43 (4) (1950) 587–599.

[13] V. Privman, D. V. Goia, J. Park, E. Matijevic, Mechanism of formation of monodispersed colloids by aggregation of nanosize precursors., J. Colloid Interf. Sci. 36 (1999) 213.

[14] J. Park, V. Privman, E. Matijevic, Model of formation of monodispersed colloids, J. Phys. Chem. B 105 (2001) 11630.

[15] S. Libert, V. Gorshkov, D. Goia, E. Matijevic, V. Privman, Model of controlled synthesis of uniform colloid particles: Cadmium sulfide, Langmuir 19 (2003) 10679–10683.